AJNR

Alterations of Microstructure and Sodium Homeostasis in Fast Amyotrophic Lateral Sclerosis Progressors: A Brain DTI and Sodium MRI Study

M.M. El Mendili, A.-M. Grapperon, R. Dintrich, J.-P Stellmann, J.-P. Ranjeva, M. Guye, A. Verschueren, S. Attarian and W. Zaaraoui

AJNR Am J Neuroradiol 2022, 43 (7) 984-990
doi: https://doi.org/10.3174/ajnr.A7559
http://www.ajnr.org/content/43/7/984

Alterations of Microstructure and Sodium Homeostasis in Fast Amyotrophic Lateral Sclerosis Progressors: A Brain DTI and Sodium MRI Study

M.M. El Mendili, A.-M. Grapperon, R. Dintrich, J.-P Stellmann, J.-P. Ranjeva, M. Guye, A. Verschueren, S. Attarian, and W. Zaaraoui

ABSTRACT

BACKGROUND AND PURPOSE: While conventional MR imaging has limited value in amyotrophic lateral sclerosis, nonconventional MR imaging has shown alterations of microstructure using diffusion MR imaging and recently sodium homeostasis with sodium MR imaging. We aimed to investigate the topography of brain regions showing combined microstructural and sodium homeostasis alterations in amyotrophic lateral sclerosis subgroups according to their disease-progression rates.

MATERIALS AND METHODS: Twenty-nine patients with amyotrophic lateral sclerosis and 24 age-matched healthy controls were recruited. Clinical assessments included disease duration and the Revised Amyotrophic Lateral Sclerosis Functional Rating Scale. Patients were clinically differentiated into fast ($n = 13$) and slow ($n = 16$) progressors according to the Revised Amyotrophic Lateral Sclerosis Functional Rating Scale progression rate. 3T MR imaging brain protocol included ^{1}H T1-weighted and diffusion sequences and a ^{23}Na density-adapted radial sequence. Quantitative maps of diffusion with fractional anisotropy, mean diffusivity, and total sodium concentration were measured. The topography of diffusion and sodium abnormalities was assessed by voxelwise analyses.

RESULTS: Patients with amyotrophic lateral sclerosis showed significantly higher sodium concentrations and lower fractional anisotropy, along with higher sodium concentrations and higher mean diffusivity compared with healthy controls, primarily within the corticospinal tracts, corona radiata, and body and genu of the corpus callosum. Fast progressors showed wider-spread abnormalities mainly in the frontal areas. In slow progressors, only fractional anisotropy measures showed abnormalities compared with healthy controls, localized in focal regions of the corticospinal tracts, the body of corpus callosum, corona radiata, and thalamic radiation.

CONCLUSIONS: The present study evidenced widespread combined microstructural and sodium homeostasis brain alterations in fast amyotrophic lateral sclerosis progressors.

ABBREVIATIONS: AD = axial diffusivity; ALS = amyotrophic lateral sclerosis; ALSFRS-R = Revised Amyotrophic Lateral Sclerosis Functional Rating Scale; ATP = adenosine triphosphate; CST = corticospinal tract; FA = fractional anisotropy; HC = healthy controls; MD = mean diffusivity; MNI152 = Montreal Neurological Institute 152; RD = radial diffusivity; TBSS = tract-based spatial statistics; TSC = total sodium concentration

Amyotrophic lateral sclerosis (ALS) is a relentlessly progressive neurodegenerative disorder leading to paralysis and ultimately death. As a heterogeneous condition, ALS is characterized by variable clinical presentations and progression of symptoms depending on various factors such as age at disease onset, the site of onset, genetic factors, and the presence of nonmotor symptoms, especially cognitive impairment.[1-4] ALS outcome varies drastically, with a median survival time from onset ranging from 24 months (Northern Europe) to 48 months (South Asia).[5] For 1.1% of cases of ALS, the median survival time from onset is 18 months and can go up to 10 years in 5%–13.3% of cases, demonstrating the heterogeneity of the disease.[3,6] While disability is commonly scored by the Revised Amyotrophic Lateral Sclerosis Functional Rating Scale (ALSFRS-R), the Amyotrophic Lateral Sclerosis Functional Rating Scale (ALSFRS) disease-progression rate is also considered an important marker of the disease to predict disability progression and patient survival.[7-9]

Conventional MR imaging (eg, T2*, FLAIR, and proton density–weighted imaging) lacks sensitivity and specificity to detect

Received January 6, 2022; accepted after revision May 10.

From the Aix Marseille University (M.M.E.M., A.-M.G., R.D., J.-P.S., J.-P.R., M.G., A.V., W.Z.), Centre National de la Recherche Scientifique, Center for Magnetic Resonance in Biology and Medicine, Marseille, France; APHM, Hopital de la Timone (M.M.E.M., A.-M.G., R.D., J.P.S., J.-P.R., M.G., A.V., W.Z.), CEMEREM, Marseille, France; and APHM, Hôpital de la Timone (A.-M.G., R.D., S.A.), Referral Centre for Neuromuscular Diseases and ALS, Marseille, France.

This research was funded by APHM (AORC Junior 2014 program), Association pour la Recherche sur la Sclérose Latérale Amyotrophique et autres maladies du motoneurone, and Fédération pour la Recherche sur le Cerveau.

Please address correspondence to Mohamed Mounir El Mendili, PhD, Centre de Résonance Magnétique Biologique et Médicale, CRMBM-CEMEREM, UMR 7339 CNRS, Aix–Marseille Université, 27 Bd Jean Moulin, 13005 Marseille, France; e-mail: mm.elmendili@univ-amu.fr

Indicates article with online supplemental data.

http://dx.doi.org/10.3174/ajnr.A7559

abnormalities in ALS and is mainly used to exclude ALS mimics.[10] Although conventional MR imaging could detect signal abnormalities in ALS such as hyperintensity in the white matter (WM) along the corticospinal tract (CST), they are rare and nonspecific and their exploration is not recommended for diagnosis.[10-13] In contrast, nonconventional MR imaging has gradually characterized features of neurodegeneration in ALS.[14] To a large extent, DTI studies have reported microstructure alterations in upper motor neurons and extramotor WM tracts.[15] Notably, DTI has shown an increased burden of WM pathology, concordant with neuropathologic staging and correlating with disease aggressiveness.[14,16-18] Recently, a sodium MR imaging study provided the first evidence of increased total sodium concentration (TSC) located in the CST of patients with ALS, reflecting disturbance of sodium homeostasis involved in metabolic failure, contributing to the neurodegenerative process.[19]

Mitochondrial dysfunction can mediate cell death by reducing adenosine triphosphate (ATP) production and impairing sodium and calcium homeostasis. If ATP availability becomes insufficient to allow ion pumps to maintain the appropriate ion gradients, changes in electrical properties and the excitability of motor neurons occur. Thus, investigating sodium concentration disturbances with sodium MR imaging could provide relevant functional information on neuron energetic status and cell viability, while DTI efficiently explores microstructural disorders. The combination of sodium and diffusion imaging could, therefore, enable the exploration of complementary processes leading to neuronal injury. Besides, one may assume that brain regions presenting combined sodium homeostasis and microstructural alterations depend on disease aggressiveness. The present study aimed to investigate the topography of brain regions showing combined microstructural and sodium homeostasis alterations in ALS subgroups according to their disease-progression rates.

MATERIALS AND METHODS

Ethics and Institutional Review Board Approval

This prospective study was approved by the local ethics committee (Comité de Protection des Personnes Sud Méditerranée 1), and written informed consent was obtained from all participants.

Study Participants and Procedures

Twenty-nine patients with ALS (9 women; mean, 54 [SD, 10] years of age; mean disease duration, 1.6 [SD, 1.2] years) were recruited from the ALS reference center of our university hospital along with 24 age- and sex-matched healthy controls (HC) with no history of neurologic or neuropsychiatric disorder (11 women; mean, 51 [SD, 11] years of age). The inclusion criteria were a diagnosis of ALS according to the revised El Escorial criteria.[20] The exclusion criteria were no current or past history of neurologic disease other than ALS, and no frontotemporal dementia, respiratory insufficiency, or substantial bulbar impairment incompatible with an MR imaging examination. Patients were clinically assessed immediately after MR imaging and scored on the ALSFRS-R.[21] Patients were clinically differentiated into fast and slow progressors according to their ALFSRS-R rate of progression, defined as ([48 ALSFRS-R]/disease duration). A threshold of 0.5 ALSFRS-R per month was set to differentiate fast from slow progressors.[22]

MR Imaging Acquisition

MR imaging was performed on a 3T Verio system (Siemens Healthineers) using a 32-channel phased-array ^{1}H head coil (Siemens Healthineers) and a ^{23}Na ^{1}H volume head coil (RAPID Biomedical).

^{1}H-MR imaging protocol included a 3D T1-weighted MPRAGE sequence (TE/TR/TI = 3/2300/900 ms, 160 slices, voxel size = $1 \times 1 \times 1$ mm^3, acquisition time = 6 minutes) and a single-shot echo-planar imaging DTI sequence (64 encoding directions, b = 1000 s/mm^2 and B_0, TE = 95 ms, TR = 10,700 ms, 60 contiguous slices, voxel size = $2 \times 2 \times 2$ mm^3, acquisition time = 12 minutes).

The ^{23}Na MR imaging protocol included a 3D density-adapted radial sequence (TR/TE = 120/0.2 ms, 17,000 projections with 369 samples per projection, voxel size = $3.6 \times 3.6 \times 3.6$ mm^3, acquisition time = 34 minutes).[23] Two tubes (50 mmol/L within 2% agar gel) placed within the FOV served as a reference for quantification.[24]

Data Processing

Anatomic. T1WIs were normalized to the Montreal Neurological Institute 152 (MNI152) template using SyN-ANTS (https://github.com/ANTsX/ANTs) nonlinear registration.[25]

DTI. Diffusion images were denoised using a local principal component analysis method that reduces signal fluctuations solely rooted in thermal noise.[26] Images were further corrected for eddy currents and head motion using affine registration to the associated non-diffusion-weighted images.[27] Fractional anisotropy (FA), mean diffusivity (MD), axial diffusivity (AD), and radial diffusivity (RD) maps were computed by fitting a tensor model.[27] FA images were aligned to the FMRIB58_FA (https://fsl.fmrib.ox.ac.uk/fsl/fslwiki/FMRIB58_FA) target, which is in MNI152 standard space, using a nonlinear registration.[27] Aligned FA images were averaged, then a "thinning" (non-maximum-suppression perpendicular to the local tract structure) was applied to create a skeletonized mean FA image. The resulting image was thresholded (FA = 0.2) to suppress areas of low mean FA values and/or high intersubject variability.[28] For each subject's FA image, the maximum FA value perpendicular to each voxel of the skeleton was projected onto the mean FA skeleton. Similarly, skeletonized MD, AD, and RD images were generated in the MNI152 space using Tract-Based Spatial Statistics (TBSS) FSL tools (https://fsl.fmrib.ox.ac.uk/fsl/fslwiki/TBSS) before voxelwise analysis.

Sodium Imaging. Sodium images were reconstructed offline, denoised, and then normalized relative to the reference tube signals to compute quantitative TSC maps of the whole brain.[19,24] TSC maps were rigidly aligned to their corresponding T1WI. Linear and nonlinear transformations were concatenated then used to bring TSC maps into the MNI152 standard space, and spatially normalized TSC maps were smoothed with a Gaussian kernel ($8 \times 8 \times 8$ mm) before voxelwise analysis.

Statistical Analysis

Statistical analysis was performed using FSL (FMRIB Software Library v6.0; https://fsl.fmrib.ox.ac.uk/fsl/fslwiki/)[27] and SPSS, Version 23 (IBM).

Demographic and clinical data[a]

	ALS	Fast	Slow	HC	*P* Value
Number	29	13	16	24	–
Age (yr)	54.3 (10.2)	56 (9.9)	52.9 (10.6)	51 (10.7)	.244[b,c] .152[b,d] .586[b,e] .388[b,f]
Sex	9F/20M	6F/7M	3F/13M	11F/13M	.394[g,c] .101[g,d] 1.000[g,e] .172[g,f]
Disease duration (mo)	18.8 (14.5)	19.4 (13.9)	18.4 (15.4)	–	–[c],–[d],–[e] .660[h,f]
Site of onset					
Spinal	22 (6 UL, 16 LL)	10 (3 UL, 7 LL)	12 (3 UL, 9 LL)	–	–
Bulbar	7	3	4	–	–
Revised El Escorial criteria					
Definite	7	7	0	–	–
Probable	7	3	6	–	–
Probable laboratory					
Supported	6	1	5	–	–
Possible	9	2	5	–	–
Disease progression rate	0.84 (0.87)	1.54 (0.93)	0.27 (0.09)	–	–[c],–[d],–[e] .001[h,f]
ALSFRS-R (/48)	38.72 (5.55)	37.31 (4.81)	40.46 (6.09)	–	–[c],–[d],–[e] .067[h,f]

Note:—F indicates female; Fast, fast progressors; LL, lower limb; M, male; mo, month; yr, year; Slow, slow progressors; –, not applicable; UL, upper limb.
[a] Values are expressed as mean (SD), unless otherwise indicated.
[b] Student *t* test.
[c] ALS versus HC.
[d] Fast versus HC.
[e] Slow versus HC.
[f] Fast versus slow.
[g] χ^2 test.
[h] Kruskal-Wallis test.

Group Comparisons. Differences in age, disease duration, and the ALSFRS-R score between groups were assessed by using the Student *t* test or the Kruskal-Wallis test when applicable. Differences in sex between groups were assessed using the χ^2 test.

Voxelwise Analysis. Differences in diffusion (FA, MD, RD, AD) and sodium (TSC) maps between groups (patients with ALS versus HC, fast versus HC, slow versus HC, fast versus slow) were assessed using permutation inference statistics (5000 permutations) combined with *t* testing. Threshold-free cluster enhancement with a significance interval of *P* values $< .05$ was used to correct for multiple comparisons (ie, family-wise error correction).[28] Common regions with significant group differences in both diffusion and TSC maps were identified from the Johns Hopkins University White Matter Tractography Atlas and labels and the Harvard-Oxford structural atlas and sorted by overlap with the corresponding tracts and cortical and subcortical regions.

RESULTS

Demographic and clinical measures of our population are reported in the Table. Figure 1 shows an example of FA and TSC images in a healthy control and fast and slow progressors. There were no significant differences in age or sex between patients with ALS and fast and slow progressors and HC (all *P* values $> .05$). There were no significant differences in disease duration or in ALSFRS-R between fast and slow progressors. The mean disease-progression rate was 1.54 (SD, 0.93) ALSFRS-R per month for fast progressors and 0.27 (SD, 0.09) ALSFRS-R per month for slow progressors.

ALS versus HC

Statistical maps resulting from voxelwise analysis and TBSS comparing patients with ALS with HC for TSC, FA, and MD are presented in Fig 2.

TSC. Patients with ALS showed significantly higher TSC compared with HC, mainly at the level of the body and genu of the corpus callosum, CSTs, bilateral corona radiata, and thalamic radiation for WM and middle frontal, precentral, postcentral, and cingulate gyri and anterior division for grey matter (GM). These clusters had a mean TSC of 58.15 (SD, 4.54) mM in patients with ALS and 53.41 (SD, 3.22) mM in HC. No clusters of significantly lower TSC in patients with ALS compared with HC were found.

DTI. Patients with ALS showed significantly lower FA compared with HC, mainly at the level of the bilateral corona radiata, body of the corpus callosum, forceps minor, genu of corpus callosum, and CSTs. Patients with ALS showed significantly higher MD compared with HC, mainly at the level of the bilateral corona radiata, body of the corpus callosum, CSTs, internal and external capsule, and longitudinal fasciculus. No clusters of significantly higher FA or lower MD in patients with ALS compared with HC were found.

Overlap between TSC and DTI. As reported in Fig 2, compared with HC, patients with ALS showed significantly higher TSC and lower FA and higher TSC and higher MD, mainly at the level of the corpus callosum, CSTs, and bilateral corona radiata. No clusters of significantly higher FA and lower TSC or lower TSC and

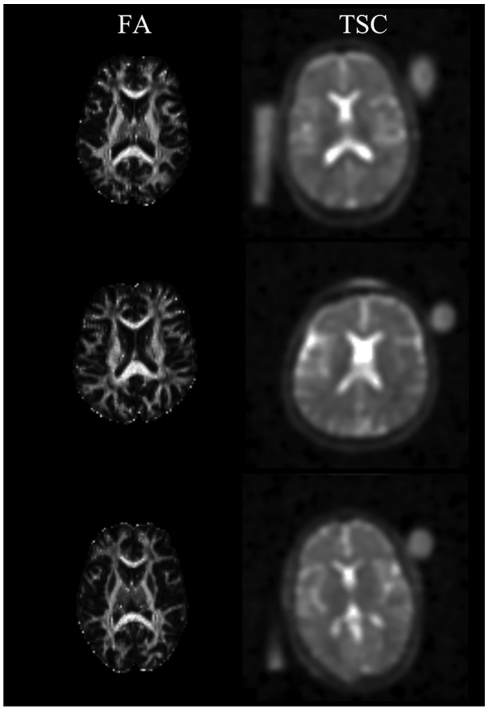

FIG 1. Example of FA and TSC maps in a healthy control (*upper row*), a fast progressor with ALS (*middle row*), and a slow progressor with ALS (*lower row*).

lower MD in those with ALS compared with HC were found. A complete list of the significant clusters emerging from the voxelwise analysis is reported in the Online Supplemental Data.

Fast Progressors versus HC

Statistical maps resulting from voxelwise analysis comparing fast ALS progressors with HC for TSC, FA, and MD are presented in Fig 3.

TSC. Fast progressors showed significantly higher TSC compared with HC, mainly at the level of the body and genu of the corpus callosum, thalamic radiation, bilateral corona radiata, forceps minor, and CSTs for WM; and precentral, postcentral, cingulate, precingulate, middle frontal, superior frontal gyri, thalamus, and caudate for GM and deep GM (Fig 3). These clusters had a mean TSC of 59.23 (SD, 5.03) mM in fast progressors and 53.12 (SD, 3.12) mM in HC. No clusters of significantly lower TSC in fast progressors compared with HC were found.

DTI. Fast progressors showed significantly lower FA compared with HC mainly in the bilateral corona radiata, body and genu of the corpus callosum, forceps minor, external capsule, uncinate fasciculus, and CSTs (Fig 3). Fast progressors showed significantly higher MD compared with HC mainly at the level of the bilateral corona radiata, body and genu of the corpus callosum, forceps minor, CSTs, internal capsule, longitudinal fasciculus, fronto-occipital fasciculus, thalamic radiation, and external capsule (Fig 3).

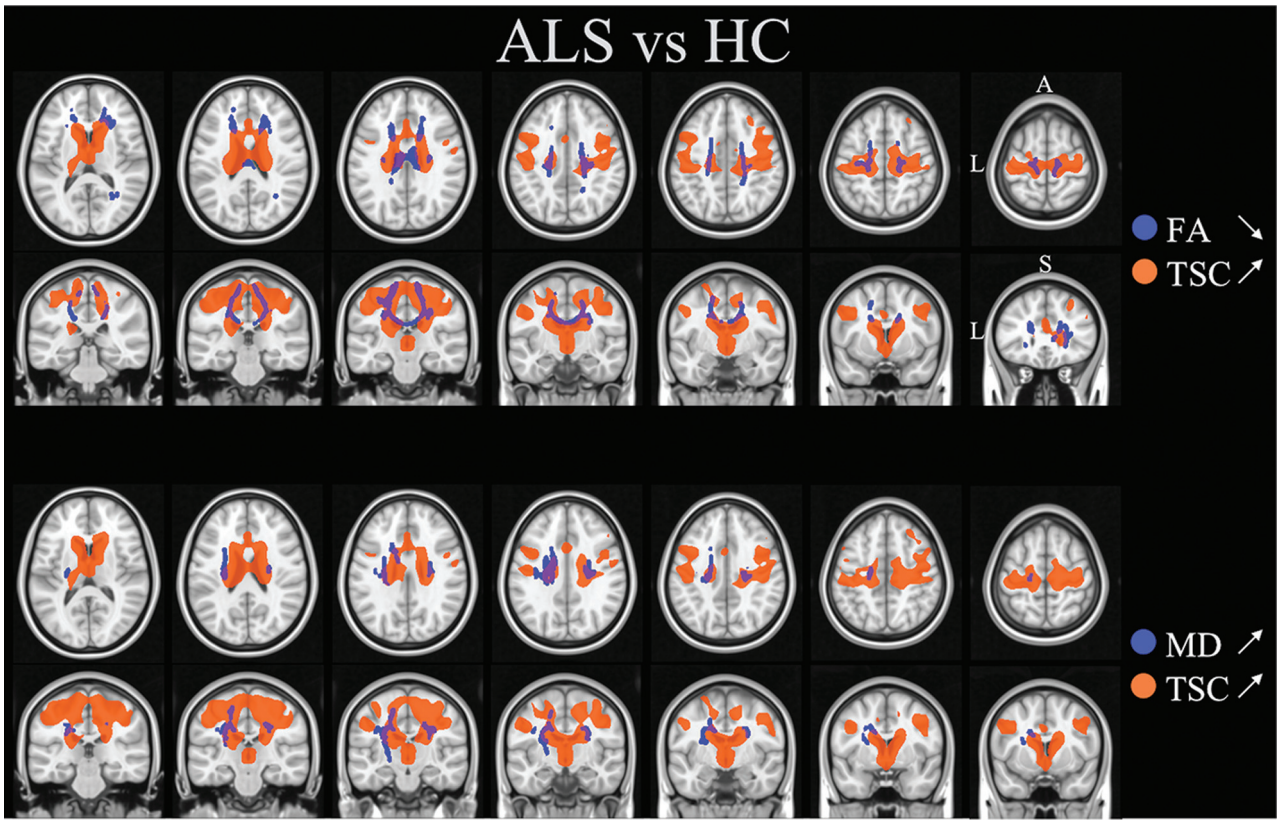

FIG 2. Significant clusters resulting from the comparison of patients with ALS and HC using voxelwise analysis of TSC (increased in ALS) and TBSS for FA (decreased in ALS) and for MD (increased in ALS). A indicates anterior; L, left; S, superior.

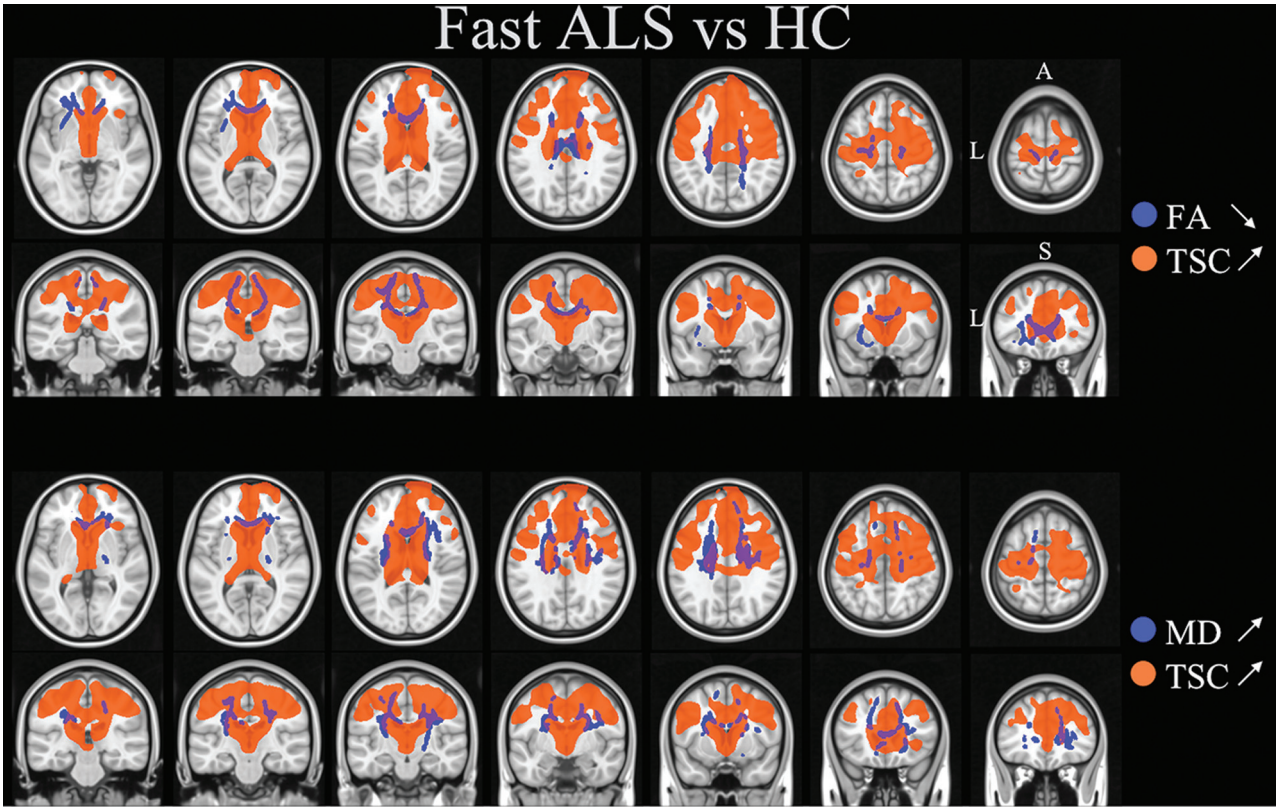

FIG 3. Significant clusters resulting from the comparison between fast ALS progressors and HC using voxelwise analysis for TSC (increased in fast ALS) and TBSS for FA (decreased in fast ALS) and MD (increased in fast ALS). A indicates anterior; L, left; S, superior.

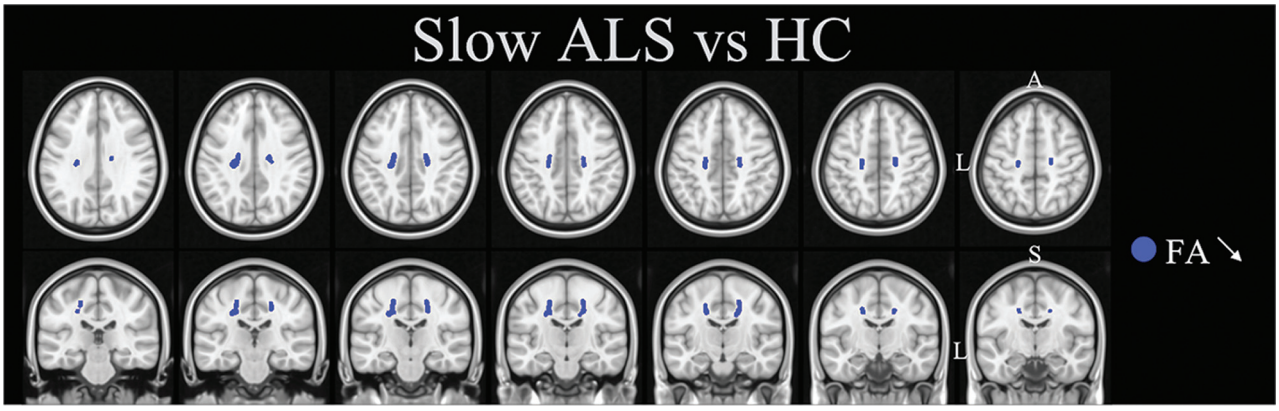

FIG 4. Significant clusters resulting from the comparison between slow ALS progressors and HC using TBSS for FA (decreased in slow ALS). A indicates anterior; L, left; S, superior.

No clusters of significantly higher FA or lower MD in fast progressors compared with HC were found.

Overlap between TSC and DTI. As reported in Fig 3, compared with HC, fast progressors showed significantly higher TSC and lower FA and higher TSC and higher MD, mainly at the level of the corona radiata, body and genu of the corpus callosum, forceps minor, and CSTs. No clusters of significantly higher FA and lower TSC or lower TSC and lower MD in fast progressors compared with HC were found. A complete list of the significant clusters emerging from the voxelwise analysis is reported in the Online Supplemental Data.

Slow Progressors versus HC

Only FA showed significantly lower values in slow progressors compared with HC, mainly at the level of the bilateral superior corona radiata, CSTs, body of the corpus callosum, and thalamic radiation (Fig 4). A complete list of the significant clusters emerging from TBSS analysis is reported in the Online Supplemental Data.

Fast versus Slow Progressors

No significant differences in TSC and DTI metrics were found between fast and slow progressors. Results from TBSS analysis for RD and AD are reported in the Online Supplemental Data.

DISCUSSION

The present study highlighted brain regions with combined microstructural and sodium homeostasis disturbances corresponding to clinically relevant regions involved in ALS, namely, the CST and the corpus callosum.[29] We opted for whole-brain voxel-to-voxel analyses to highlight the focal tissue involvement that would be masked by a global approach such as an ROI. Our results are in accordance with DTI studies that confirmed the impairment of the CST (subcortical to brainstem) as a main hallmark in ALS, even in patients with no upper motor neuron signs at the time of MR imaging but who developed pyramidal symptoms later.[16,30,31] Furthermore, callosal impairment has also been stressed by several studies, especially the motor-related regions of the corpus callosum.[10,32] A recent meta-analysis DTI study analyzing 14 studies with 396 patients with ALS reported 2 clusters of brain microstructural impairment.[33] The first cluster was located in the left corona radiata, extending to the body and splenium of the corpus callosum, left superior longitudinal fasciculus, posterior limb of the internal capsule, right corona radiata, and bilateral cingulate gyrus. The second cluster was located in the right corticospinal tract, which extended to the right cerebral peduncle. Most interesting, these 2 clusters were found in our study to be the site of microstructural impairment but also sodium homeostasis disturbances, a marker of neurodegeneration related to mitochondrial dysfunction and energy failure.[19-34]

Considering that heterogeneous disease-progression rates impact prognosis and might affect the responsiveness to future treatments, there has been recent effort to study patient stratification.[35,36] Stratifying patients by disease progression, we characterized widespread, combined microstructural and ionic alterations in fast progressors, while slow progressors showed only restricted microstructure damage. These results are important because they reflect diverse pathophysiologic processes in patients with no difference in age or disease duration or disability scale (ALSFRS-R) but who experienced different disease-progression rates. A few studies have investigated WM and GM alterations in fast and slow progressors.[16,17,30] A DTI study reported that fast progressors with lower-motor-neuron ALS had a substantial impairment in the CST and frontal and prefrontal brain regions compared with HC, while slow progressors showed less severe alterations.[17] In addition, patients with high disease aggressiveness showed a distinct pattern of supratentorial WM density decreases relative to those with low aggressiveness but no significant differences in GM density suggesting axonal loss.[30]

In our study, we found sodium alterations that reflect mitochondrial dysfunction and subsequent energy failure, both of which are key factors in the induction of pathologic processes in ALS.[37,38] In vitro experiments demonstrated that axonal degeneration caused by experimental anoxia within the brain is a calcium ion (Ca^{2+})-dependent process that can be triggered by a sustained sodium ion (Na+) influx driving reverse Na^+–Ca^{2+} exchange and importing damaging levels of Ca^{2+} within the axons.[39] This early work suggested that ATP depletion and consequent Na^+-(potassium) K^+-ATPase failure might result in a breakdown of ionic gradients because Na^+ ions enter the axon via persistently activated Na+ channels. An additional study reported that axons may degenerate because nitric oxide (NO) can inhibit mitochondrial respiration, resulting in energy failure and intra-axonal accumulation of sodium. Most interesting, axons could be protected from NO-mediated damage by using Na^+ channel blockers.[40]

Limitations

The cross-sectional design of the study did not allow us to assess the course of the disease between fast and slow progressors and investigate whether fast progressors are an ALS phenotype, as suggested in some studies,[16,17] or a maladaptive condition. In the present study, fast and slow progressors were differentiated using a threshold of 0.47 for the disease-progression rate. This choice was based on the results of a previous study,[22] which found that this threshold was a significant predictor of survival in ALS. Nevertheless, because no consensus is available, this may be open to discussion. Another limitation is related to the restricted number of patients, which prevented better staging between subgroups and might explain the lack of a significant difference between fast and slow progressors. Finally, a neuropsychological assessment would have helped to explain whether clusters found in the frontotemporal lobe of fast progressors were due to cognitive deficits. Future multicentric and longitudinal imaging studies will be of interest to identify early markers of neurodegeneration and predict the course of the disease of individual patients.[41]

CONCLUSIONS

The present brain DTI and sodium MR imaging study evidenced combined microstructural and sodium homeostasis alterations in ALS. These alterations were in accordance with disease aggressiveness. Fast progressors showed more widespread brain tissue damage than slow progressors compared with HC. Our study highlights the relevance of a multinuclear MR imaging approach to stratify patients according to their disease aggressiveness.

Disclosure forms provided by the authors are available with the full text and PDF of this article at www.ajnr.org.

REFERENCES

1. Chiò A, Moglia C, Canosa A, et al. **Cognitive impairment across ALS clinical stages in a population-based cohort.** *Neurology* 2019;93:e984–94 CrossRef Medline
2. Chiò A, Logroscino G, Traynor BJ, et al. **Global epidemiology of amyotrophic lateral sclerosis: a systematic review of the published literature.** *Neuroepidemiology* 2013;41:118–30 CrossRef Medline
3. Chiò A, Calvo A, Moglia C, et al; PARALS Study Group. **Phenotypic heterogeneity of amyotrophic lateral sclerosis: a population-based study.** *J Neurol Neurosurg Psychiatry* 2011;82:740–46 CrossRef Medline
4. Volk AE, Weishaupt JH, Andersen PM, et al. **Current knowledge and recent insights into the genetic basis of amyotrophic lateral sclerosis.** *Med Genet* 2018;30:252–58 CrossRef Medline
5. Marin B, Boumédiene F, Logroscino G, et al. **Variation in worldwide incidence of amyotrophic lateral sclerosis: a meta-analysis.** *Int J Epidemiol* 2017;46:57–74 CrossRef Medline
6. Pupillo E, Messina P, Logroscino G, et al; SLALOM Group. **Long-term survival in amyotrophic lateral sclerosis: a population-based study.** *Ann Neurol* 2014;75:287–97 CrossRef Medline
7. Kimura F, Fujimura C, Ishida S, et al. **Progression rate of ALSFRS-R at time of diagnosis predicts survival time in ALS.** *Neurology* 2006;66:265–67 CrossRef Medline
8. Kollewe K, Mauss U, Krampfl K, et al. **ALSFRS-R score and its ratio: a useful predictor for ALS-progression.** *J Neurol Sci* 2008;275:69–73 CrossRef Medline

9. Daghlas SA, Govindarajan R; Pooled Resource Open-Access ALS Clinical Trials Consortium. **Relative effects of forced vital capacity and ALSFRS-R on survival in ALS.** *Muscle Nerve* 2021;64:346–51 CrossRef Medline
10. Filippini N, Douaud G, Mackay CE, et al. **Corpus callosum involvement is a consistent feature of amyotrophic lateral sclerosis.** *Neurology* 2010;75:1645–52 CrossRef Medline
11. Winhammar JM, Rowe DB, Henderson RD, et al. **Assessment of disease progression in motor neuron disease.** *Lancet Neurol* 2005;4:229–38 CrossRef Medline
12. Gupta A, Nguyen TB, Chakraborty S, et al. **Accuracy of conventional MRI in ALS.** *Can J Neurol Sci* 2014;41:53–57 CrossRef Medline
13. Jin J, Hu F, Zhang Q, et al. **Hyperintensity of the corticospinal tract on FLAIR: a simple and sensitive objective upper motor neuron degeneration marker in clinically verified amyotrophic lateral sclerosis.** *J Neurol Sci* 2016;367:177–83 CrossRef Medline
14. Kassubek J, Müller HP. **Advanced neuroimaging approaches in amyotrophic lateral sclerosis: refining the clinical diagnosis.** *Expert Rev Neurother* 2020;20:237–49 CrossRef Medline
15. Basaia S, Filippi M, Spinelli EG, et al. **White matter microstructure breakdown in the motor neuron disease spectrum: recent advances using diffusion magnetic resonance imaging.** *Front Neurol* 2019;10:193 CrossRef Medline
16. Steinbach R, Gaur N, Roediger A, et al. **Disease aggressiveness signatures of amyotrophic lateral sclerosis in white matter tracts revealed by the D50 disease progression model.** *Hum Brain Mapp* 2021;42:737–52 CrossRef Medline
17. Müller HP, Agosta F, Riva N, et al. **Fast progressive lower motor neuron disease is an ALS variant: a two-centre tract of interest-based MRI data analysis.** *Neuroimage Clin* 2018;17:145–52 CrossRef Medline
18. Brettschneider J, Del Tredici K, Toledo JB, et al. **Stages of pTDP-43 pathology in amyotrophic lateral sclerosis.** *Ann Neurol* 2013;74:20–38 CrossRef Medline
19. Grapperon AM, Ridley B, Verschueren A, et al. **Quantitative brain sodium MRI depicts corticospinal impairment in amyotrophic lateral sclerosis.** *Radiology* 2019;292:422–28 CrossRef Medline
20. Brooks BR, Miller RG, Swash M, et al; World Federation of Neurology Research Group on Motor Neuron Diseases. **El Escorial revisited: revised criteria for the diagnosis of amyotrophic lateral sclerosis.** *Amyotroph Lateral Scler Other Motor Neuron Disord* 2000;1:293–99 CrossRef Medline
21. Cedarbaum JM, Stambler N, Malta E, et al. **The ALSFRS-R: a revised ALS functional rating scale that incorporates assessments of respiratory function—BDNF ALS Study Group (Phase III).** *J Neurol Sci* 1999;169:13–21 CrossRef Medline
22. Labra J, Menon P, Byth K, et al. **Rate of disease progression: a prognostic biomarker in ALS.** *J Neurol Neurosurg Psychiatry* 2016;87:628–32 CrossRef Medline
23. Nagel AM, Laun FB, Weber MA, et al. **Sodium MRI using a density-adapted 3D radial acquisition technique.** *Magn Reson Med* 2009;62:1565–73 CrossRef Medline
24. Ridley B, Marchi A, Wirsich J, et al. **Brain sodium MRI in human epilepsy: disturbances of ionic homeostasis reflect the organization of pathological regions.** *Neuroimage* 2017;157:173–83 CrossRef Medline
25. Avants BB, Tustison NJ, Stauffer M, et al. **The Insight ToolKit image registration framework.** *Front Neuroinform* 2014;8:44 CrossRef Medline
26. Manjón JV, Coupé P, Concha L, et al. **Diffusion weighted image denoising using overcomplete local PCA.** *PLoS One* 2013;8:e73021 CrossRef Medline
27. Jenkinson M, Beckmann CF, Behrens TE, et al. **FSL.** *Neuroimage* 2012;62:782–90 CrossRef Medline
28. Smith SM, Jenkinson M, Johansen-Berg H, et al. **Tract-Based Spatial Statistics: voxelwise analysis of multi-subject diffusion data.** *Neuroimage* 2006;31:1487–505 CrossRef Medline
29. Bede P, Iyer PM, Schuster C, et al. **The selective anatomical vulnerability of ALS: "disease-defining" and "disease-defying" brain regions.** *Amyotroph Lateral Scler Frontotemporal Degener* 2016;17:561–70 CrossRef Medline
30. Steinbach R, Prell T, Gaur N, et al. **Patterns of grey and white matter changes differ between bulbar and limb onset amyotrophic lateral sclerosis.** *Neuroimage Clin* 2021;30:10267 CrossRef Medline
31. Sach M, Winkler G, Glauche V, et al. **Diffusion tensor MRI of early upper motor neuron involvement in amyotrophic lateral sclerosis.** *Brain* 2004;127:340–50 CrossRef Medline
32. Chapman MC, Jelsone-Swain L, Johnson TD, et al. **Diffusion tensor MRI of the corpus callosum in amyotrophic lateral sclerosis.** *J Magn Reson Imaging* 2014;39:641–47 CrossRef Medline
33. Zhang F, Chen G, He M, et al. **Altered white matter microarchitecture in amyotrophic lateral sclerosis: a voxel-based meta-analysis of diffusion tensor imaging.** *Neuroimage Clin* 2018;19:122–29 CrossRef Medline
34. Huhn K, Engelhorn T, Linker RA, et al. **Potential of sodium MRI as a biomarker for neurodegeneration and neuroinflammation in multiple sclerosis.** *Front Neurol* 2019;10:84 CrossRef Medline
35. Schuster C, Hardiman O, Bede P. **Survival prediction in amyotrophic lateral sclerosis based on MRI measures and clinical characteristics.** *BMC Neurol* 2017;17:73 CrossRef Medline
36. Spinelli EG, Riva N, Rancoita PMV, et al. **Structural MRI outcomes and predictors of disease progression in amyotrophic lateral sclerosis.** *Neuroimage Clin* 2020;27:102315 CrossRef Medline
37. Sassani M, Alix JJ, McDermott CJ, et al. **Magnetic resonance spectroscopy reveals mitochondrial dysfunction in amyotrophic lateral sclerosis.** *Brain* 2020;143:3603–18 CrossRef Medline
38. Vandoorne T, De Bock K, Van Den Bosch L. **Energy metabolism in ALS: an underappreciated opportunity?** *Acta Neuropathol* 2018;135:489–509 CrossRef Medline
39. Stys PK, Waxman SG, Ransom BR. **Ionic mechanisms of anoxic injury in mammalian CNS white matter: role of Na+ channels and Na(+)-Ca2+ exchanger**. *J Neurosci* 1992;12:430–39 CrossRef Medline
40. Kapoor R, Davies M, Blaker PA, et al. **Blockers of sodium and calcium entry protect axons from nitric oxide-mediated degeneration.** *Ann Neurol* 2003;53:174–80 CrossRef Medline
41. Meier JM, van der Burgh HK, Nitert AD, et al. **Connectome-based propagation model in amyotrophic lateral sclerosis.** *Ann Neurol* 2020;87:725–38 CrossRef Medline